Electronic Supplementary Information for "Correlation between Magnetic-microstructure and Microwave Mitigation Ability of $M_xCo_{(1-x)}Fe_2O_4$ (M: Ni^{2+}, Mn^{2+}, Zn^{2+}) based Ferrite-Carbon Black/PVA Composites"

Gopal Datt and A. C. Abhyankar*,

Department of Materials Engineering, Defence Institute of Advanced Technology, Girinagar, Pune-411025, India.

*Corresponding Author Address:

Tel. No.: +91-20-24304311,

Email: ashutoshabhyankar@gmail.com

Figure-S1: Schematics for the synthesis procedure of ferrite and ferrite-carbon Hybrid.

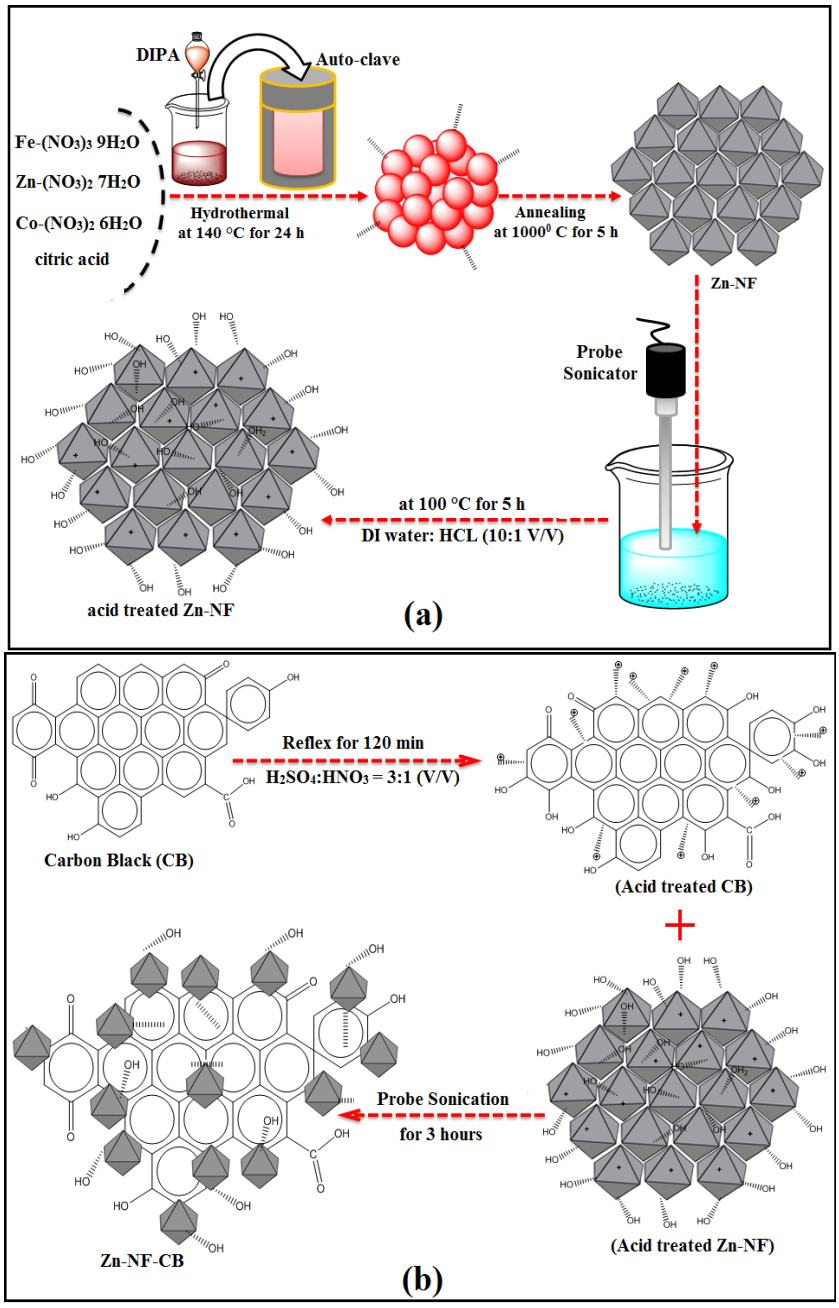

Figure-S1: (a) Schematic for the hydrothermal synthesis procedure of Zn-NF and acid treated Zn-NF and (b) Schematic for the synthesis procedure of Zn-NF-CB hybrid.

Preparation of NF-CB hybrids and flexible NF-CB/PVA composite films:

At first, the CB was refluxed with concentrated mineral acid (which is 3:1 (v/v) mixture of H_2SO_4 and HNO_3) for 2 hours and was rinsed with deionized water and dried. The NFs too were treated with Hydrochloric acid (HCL, 39%, analytical grade). The mixture of acid-

treated NFs of different weight percentage (10 wt. %, 15 wt. %, 20 wt. % and 25 wt. %) and CB was sonicated for 3 hours (with a probe sonicator at a speed of 25,000 rpm) under nitrogen (N_2) (for sample codes and details see table-1). The final NF-CB solution was transferred to the Teflon autoclave and was heated for 10 hour at 100 °C. The black NF-CB hybrids were centrifuged and washed several times with ethanol and finally it were dried at 50°C for 12 hours in vacuum. The synthesis of NF-CB hybrids is illustrated in figure-S1 (b) of the supplementary sheet.

Figure S2: FESEM micrographs of all three nano-ferrites (NFs).

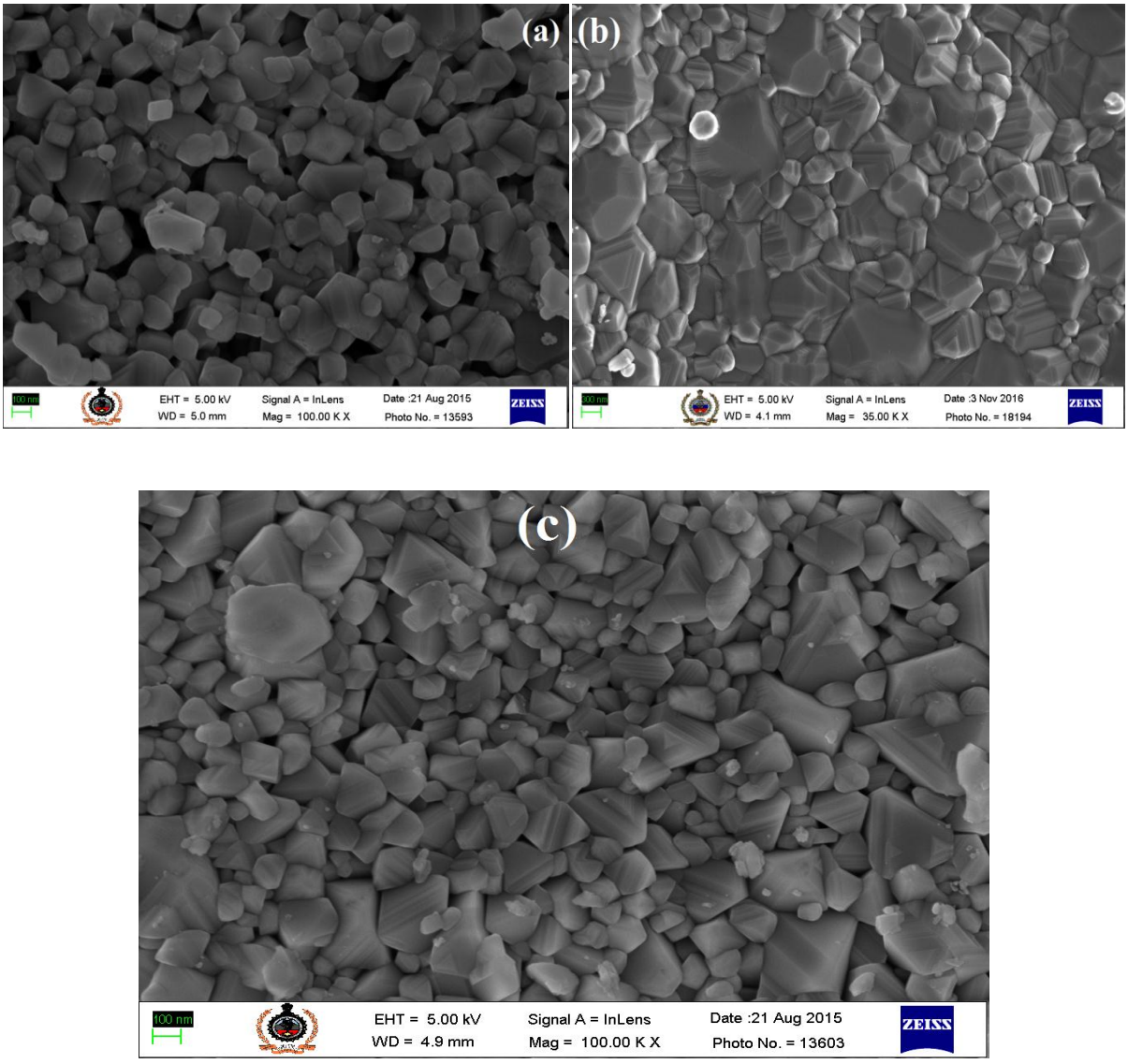

Figure S2: FESEM micrographs of all three NFs: (a) Mn-NF, (b) Ni-NF and (c) Zn-NF respectively.

Figure S3: EDX spectrum and percentage of different elements (in insert table) of (a) Mn-NF (b) Ni-NF and (c) Zn-NF.

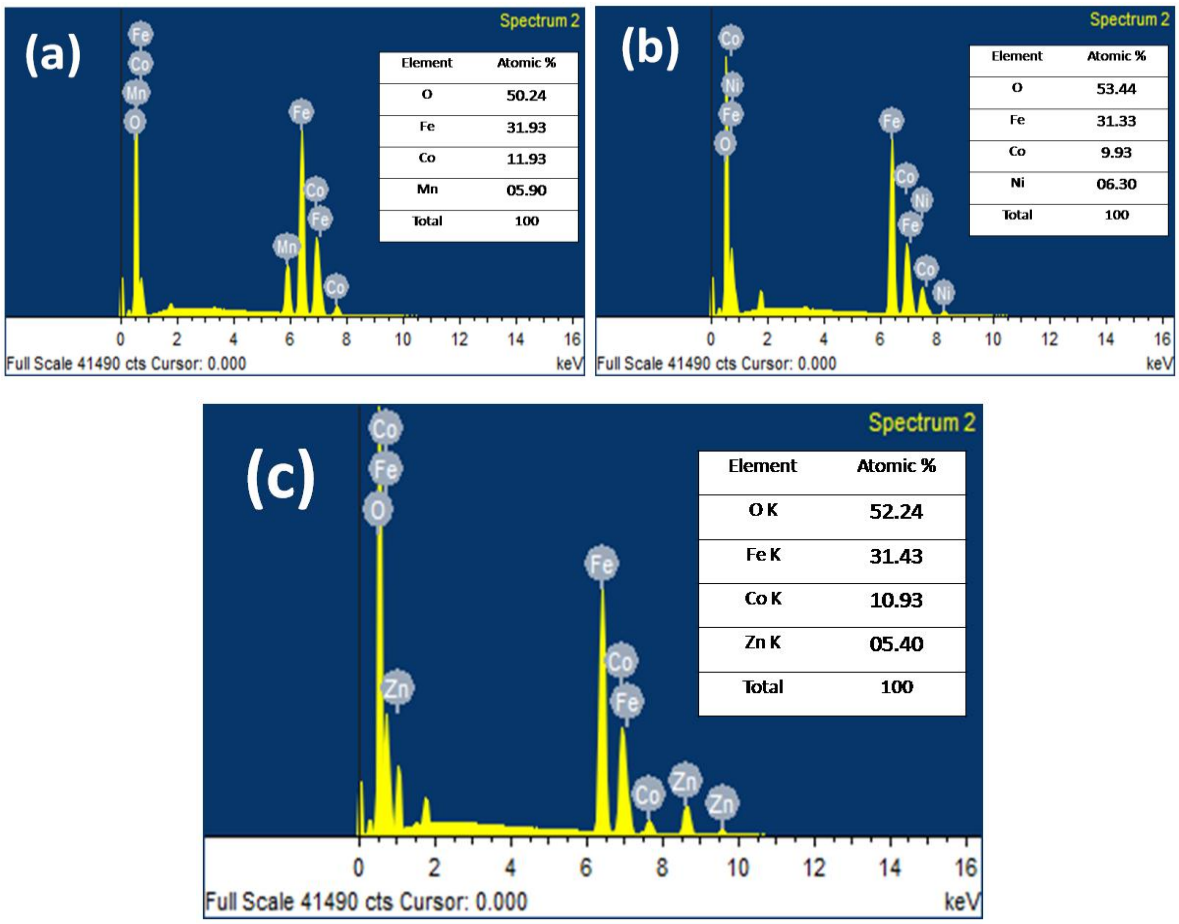

Figure S3: EDX spectrum and percentage of different elements (in insert table) of (a) Mn-NF (b) Ni-NF (c) Zn-NF.

Dielectric properties of Zn-NF-CB/PVA composite with different wt% of Zn-NF

The effect of weight percentage (wt %) of ferrite on electrical conductivity of NF/CB hybrid and NF-CB/PVA composite is important. We have measured ac electrical conductivity and dielectric permeability of different wt % ferrite based composites. The weight percentage of carbon black was kept fixed at 15 wt% while the weight percentage of Zn-NF ferrite has been varied from 0 to 25 wt % as 10 wt%, 15 wt%, 20 wt% and 25 wt%. The real part of ac conductivity of all Zn-NF-CB/PVA composites is illustrated in figure-S4 (a) over the frequency range of 1 Hz to 1 MHz. Figure-S4 (a) indicates that increase in the amount of Zn-NF in Zn-NF-CB/PVA composite, the real part of ac conductivity (σ') decreases. This decrease can be attributed to weakening of interconnected conducting network of carbon black particles in the composite due to incorporating ferrite particles that are semiconducting.

For 25 wt% Zn-NF loading in Zn-NF-CB/PVA composite, conductivity again starts increasing. This increase indicates that after reaching the critical loading percentage, electron hopping between Zn-NF and other constituents enhances significantly and it contributes to electric conductivity of composite. Therefore, 25 wt% loading can be considered as an optimal loading percentage, which will be applied to further study of dielectric and EM wave absorption properties. However, for a good EM wave absorbing composite, primary requirement is not of high electrical conductivity but of interconnected network of different constituents and a conduction path. For a good EM wave absorber, dielectric and magnetic properties are considered important. Therefore, the effect of NF wt% loading on dielectric properties of NF-CB/PVA composites is studied along with compositional dependent of dielectric properties.

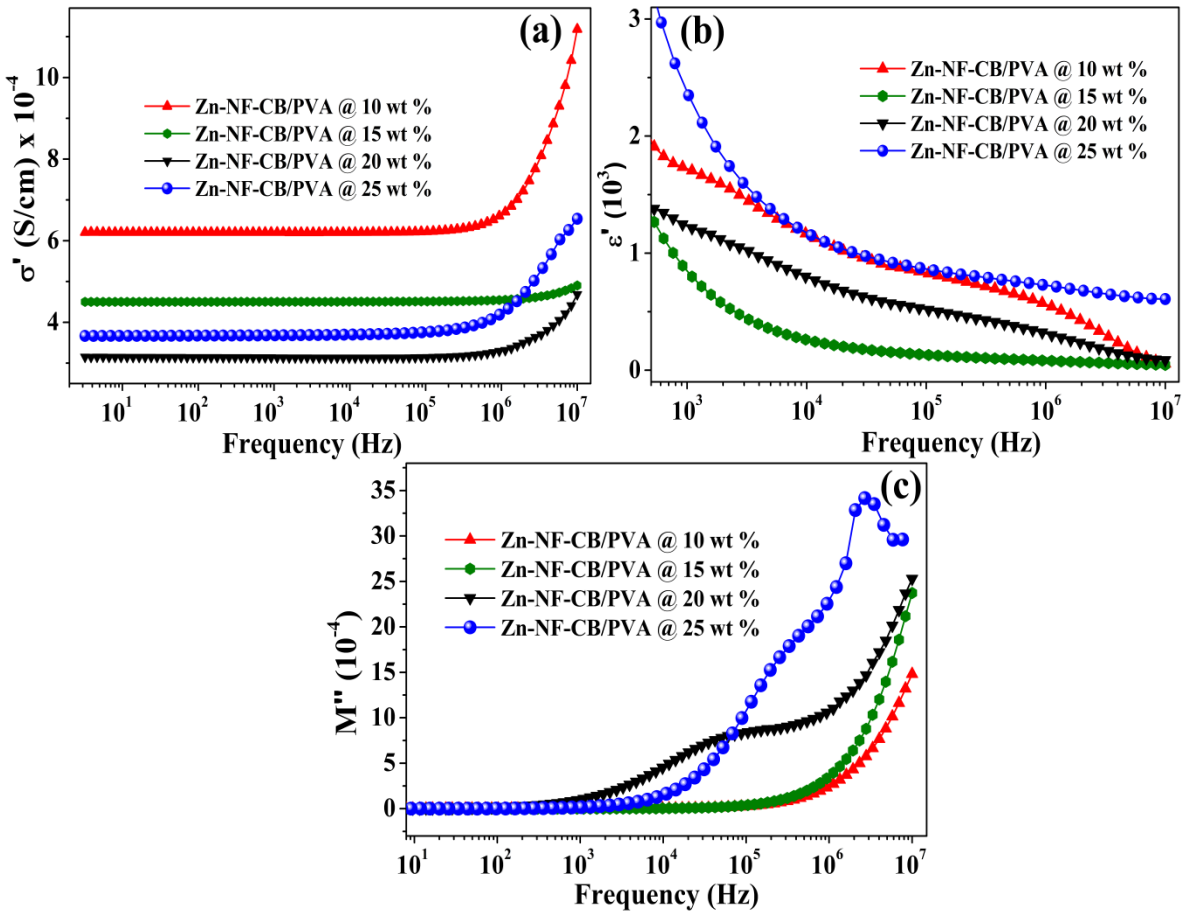

Figure-S4: (a) The real part of AC electrical conductivity (σ') of Zn-NF-CB/PVA composite with different wt% of Zn-NF; (b) The permittivity (ε') of the Zn-NF-CB/PVA composite with different wt% of Zn-NF; (c) The imaginary part of electric modulus (M'') Zn-NF-CB/PVA composite with different wt% of Zn-NF respectively.

Figure-S4 (b) illustrates the real part of dielectric permittivity (ε') for Zn-NF-CB/PVA composite with different wt. % of Zn-NF (10 wt%, 15 wt%, 20 wt% and 25 wt %). On increasing the wt% of Zn-NF in Zn-NF-CB/PVA composite, dielectric permittivity initially decreased on going from 10 wt% to 15 wt% of Zn-NF loading and increased later. The 25 wt % composite shows the maximum dielectric permittivity (see figure-S4 b). This type of manifold enhancement in dielectric constant was reported near percolation threshold in a composite[1]. Therefore, 25 wt% of NF in Zn-NF-CB/PVA composite can be roughly considered as the (or nearly) optimal loading of NF.

Table-S1: The AC electrical conductivity and dielectric permittivity of different samples.

Samples Name	**wt% of NF in the NF-CB/PVA composite**	**σ' (S/cm^{-1}) At 1 MHz**	**ε' at 1 MHz**
CB/PVA	0 wt% of Zn-NF	1.02 x10^{-3}	206
Zn-NF-CB/PVA	25 wt% of Zn-NF	4.33 x10^{-4}	713
Mn-NF-CB/PVA	25 wt% of Mn-NF	1.66 x10^{-4}	230
Ni-NF-CB/PVA	25 wt% of Ni-NF	1.66 x10^{-5}	35

Table-S2: The different sample codes and description of their constituents.

Sample Name	**Description of constituents**
Zn-NF/PVA	25wt% Zn-NF NPs in 2 g of PVA
CB/PVA	15 wt% CB in 2 g of PVA
Zn-NF-CB/PVA	15 wt% CB and 25 wt% Zn-NF in 2 g of PVA
Mn-NF-CB/PVA	15 wt% CB and 25 wt% Mn-NF in 2 g of PVA
Ni-NF-CB/PVA	15 wt% CB and 25 wt% Ni-NF in 2 g of PVA

Initially incorporation of Zn-NF particles in composite films weakens the conducting network, which leads to decrease in surface charge polarization and consequently decrease in dielectric permittivity. However, dielectric permittivity increases after 20 wt% of Zn-NF particles in Zn-NF-CB/PVA composite. It could be due to the enhancement in interfacial polarization since with more number of Zn-NF particles, there will be increase in equal proportion of total number of Zn-NF-CB and Zn-NF/PVA interface. The increase in permittivity after 20 wt% loading of Zn-NF confirms that the interfacial polarization becomes dominant polarization. For Zn-NF-

CB/PVA composite with varying Zn-NF wt%, the imaginary part of electric modulus, M'' is shown in figure-S4 (c). The electric modulus is[2]:

$$M = M' + jM'' = \frac{1}{\varepsilon^*} = \frac{1}{\varepsilon' - j\varepsilon''} = \frac{\varepsilon'}{\varepsilon'^2 + \varepsilon''^2} + j\frac{\varepsilon''}{\varepsilon'^2 + \varepsilon''^2} \quad (S1)$$

where ε' and ε'' are the real and imagery part of dielectric permittivity and $j = \sqrt{-1}$. The electric modulus M'' shows a broad intense peak for 20 wt% and 25 wt% of Zn-NF loading (figure-S4 c). On increasing Zn-NF wt% from 20 to 25, this peak becomes broader, more intense, and shifts toward higher frequency. It can be attributed to enhancement in interfacial polarization (Maxwell–Wagner–Sillars type polarization) in 20 wt% and 25 wt% (of Zn-NF) Zn-NF-CB/PVA composites[2]. This interfacial polarization arises when two different constituents of a dielectric/magnetic media heterostructure differ in electrical conductivity or dielectric permittivity (heterogeneous interface)[3, 4]. Due to difference in electrical conductivity at the interface of these two constituent (in present case CB/Ferrite particles, ferrite/PVA and CB/PVA are the main interfaces), virtual electric charge, which is responsible for interfacial polarization, gets accumulate at the interface. Therefore, in case of 20 wt% and 25 wt% of Zn-NF loaded Zn-NF-CB/PVA composite, interfacial polarization can be considered as main dielectric relaxation mechanism that dominates dielectric properties.

Shielding Effectiveness of Zn-NF-CB/PVA composite with different wt% of Zn-NF

Figure-S5 (a) illustrates frequency dependence of total shielding effectiveness (SE) of Zn-NF-CB/PVA composite in the frequency range of 8-18 GHz (X and Ku-band). A series of experiments were conducted to investigate the effect of wt% of NF on microwave absorption. In Zn-NF-CB/PVA composite, wt% of Zn-NF is varied from 0 wt% to 25 wt% i.e. 0 wt%, 10 wt%, 15 wt%, 20 wt% and 25 wt% (see table-1) while wt% of CB is fixed at 15 wt%. The total shielding effectiveness (SE) increased from 12 dB to 32 dB with increasing wt% of Zn-NF in Zn-NF-CB/PVA composite. (see figure- S5 a). Figure- S5 (b) and S5 (c) illustrates the shielding due to absorption (SE_A) and reflection (SE_R) respectively as a function of frequency for different wt% of Zn-NF. SE_A increases monotonically from 8 dB to 27 dB on increasing the wt% of Zn-NF and the dominant shielding mechanism is absorption. The CB/PVA film (composite without ferrite filler or 0 wt% ferrite) has approximately 13 dB of SE. Hence, synergetic effect between Zn-NF, CB and PVA can also be considered important in absorption mechanism[5]. This enhancement in SE of Zn-NF-CB/PVA composite can be mainly due to enhancement in interfacial polarization because of increase in number of interfaces, enhancement in surface charge polarization and conduction losses, and magnetic

losses due to the magnetic nature of Zn-NF through various magnetic losses mechanism, which will be discussed later.

For above 20 wt% of Zn-NF in composite, SE is above 20 dB (99.5 % attenuation of EM wave), which is necessary for commercial level applications. Therefore, composites above 20 wt% of Zn-NF loading can be used as efficient microwave absorber. Zn-NF-CB/PVA composites with 25 wt% of Zn-NF exhibits the highest total shielding effectiveness of ~32-35 dB (more than 99.99 % attenuation of EM wave) with absorption as dominant EM wave attenuation mechanism. For further study, 25 wt% of nano-ferrites (NF) in NF-CB/PVA nanocomposites will be considered as an optimal percentage for all three composite samples and henceforth composite with 25 wt% loading of NF will be referred. In the next section we will investigate effect of these three different types of nano-ferrite on EM wave shielding properties of NF-CB/PVA composite.

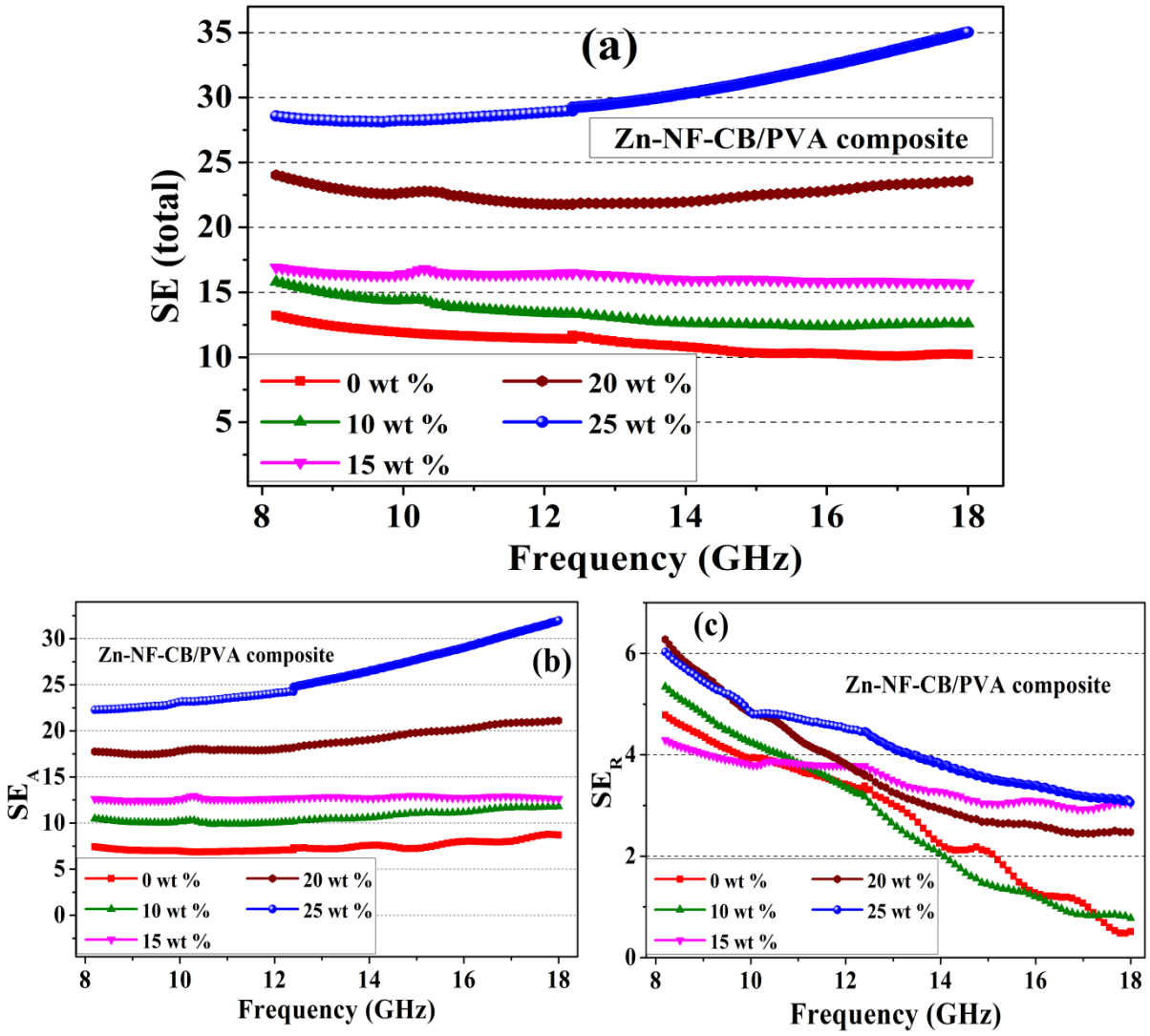

Figure-S5: (a) Total shielding effectiveness (SE), (b) shielding due to absorption (SE_A) and (c) shielding due to reflection (SE_R) respectively of Zn-NF-CB/PVA composite films with different weight percentage of Zn-NF (0 wt%, to 25 wt%), in 8-18 GHz range.

Magnetic Properties of Nano-ferrites (NFs) and NF-CB/PVA composite: The magnetization curves for the NFs, namely Mn-NF, Ni-NF and Zn-NF, at 300 K are shown in Figure-S6. The magnetization data analysis of these samples shows that, the Mn-NF ($Mn_{0.4}Co_{0.6}Fe_2O_4$) sample has the highest saturation magnetization. Furthermore we have also recorded the magnetization curve for all the composite samples with an applied field up to 8 Tesla and they are presented in the Figure-S6 below. It can be seen from the figure that, amongst all three composites, the Zn-NF-CB/PVA composite samples shows the highest magnetization (16 emu/g). The magnetization value of Mn-NF-CB/PVA samples is found to be lower (12 emu/g), which due to the fact that after fabricating composite of Mn-NF with CB and PVA, the exchange coupling between the adjacent Mn-NF particles is weaken greatly in Mn-NF-CB/PVA samples.

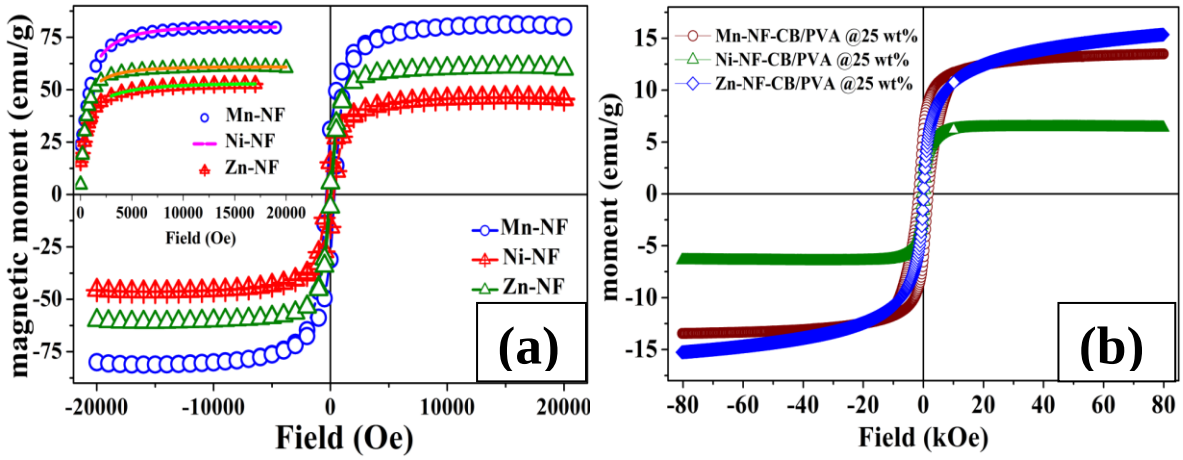

Figure-S6: M-H curve at 300 K for: (a) all three NFs and (b) for all three composite samples.

AFM, MFM and Schematic Representation of Spins in NFs:

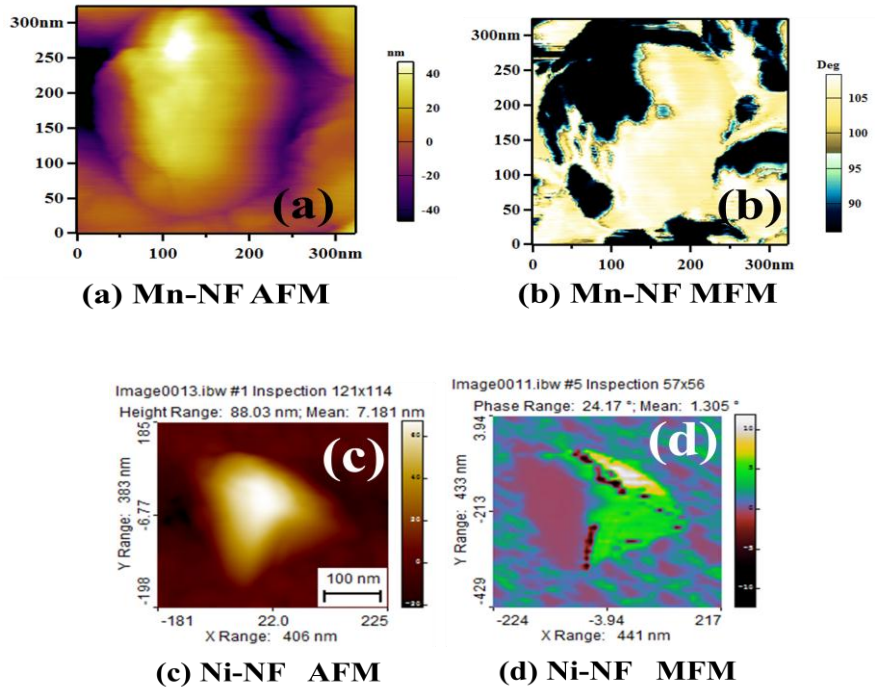

Figure-S7: (a) The AFM topographic and (b) Magnetic phase image (MFM) of: (a, b) Mn-NFs and (c, d) Ni-NFs, respectively.

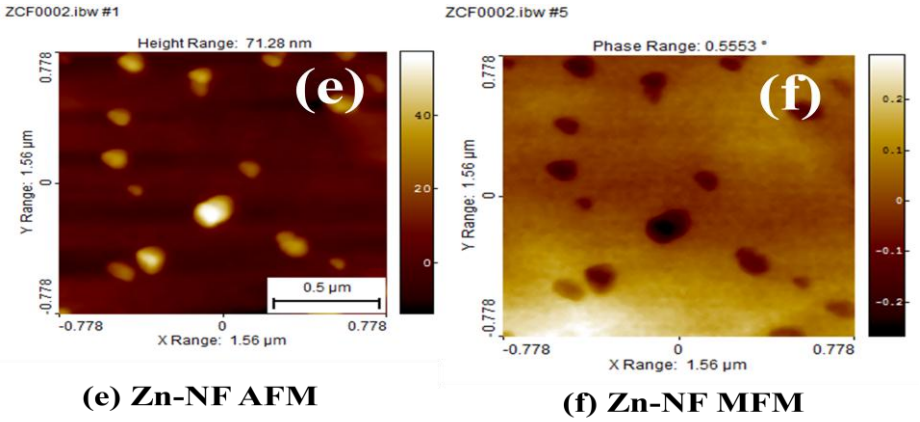

Figure-S7: (e) The AFM topographic and (f) Magnetic phase image (MFM) of number of Zn-NFs particles, respectively with colour scale.

XRD data along with Rietveld fit (in solid lines) of all three NF:

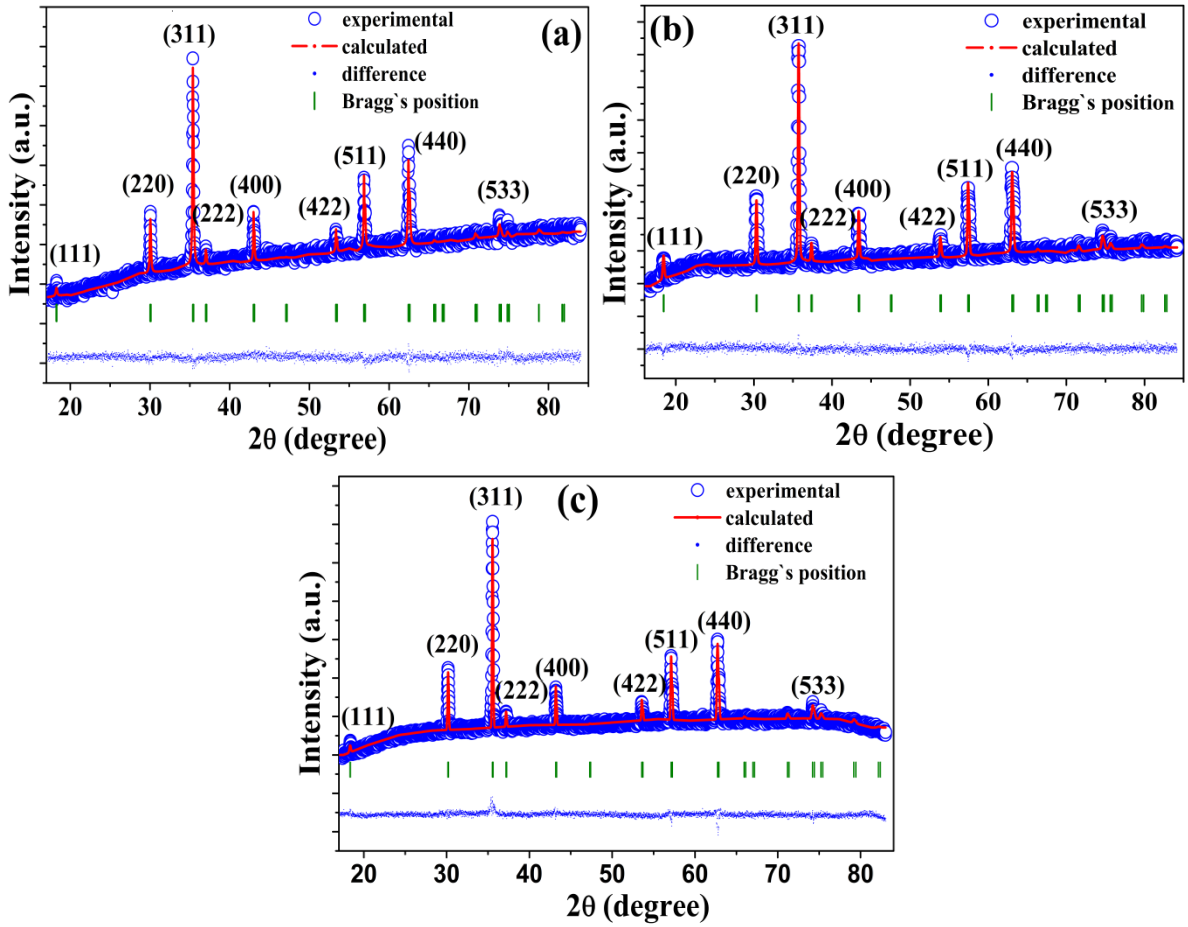

Figure-S8: XRD data, Rietveld fit (in solid lines) and the difference curve of (a) Mn-NF (b) Ni-Zn and (c) Zn-NF.

References:

1. Nan, C-W., Y. Shen, and Jing Ma. "Physical properties of composites near percolation." Annual Review of Materials Research 40 (2010): 131-151.
2. Wu, Wei, Xingyi Huang, Shengtao Li, Pingkai Jiang, and Tanaka Toshikatsu. "Novel three-dimensional zinc oxide superstructures for high dielectric constant polymer composites capable of withstanding high electric field." *J. Phys. Chem. C*, **2012**, 116, 24887-24895.
3. Zhang, X.; Li, Y.; Liu, R.; Rao, Y.; Rong, H.; Qin, G. “High Magnetization FeCo Nano-chains with Ultrathin Interfacial Gaps for Broadband Electromagnetic Wave Absorption at Gigahertz.” *ACS Appl. Mater. Interfaces.* **2016**, 8, 3494−3498.

4. Vyas, Manoj Kumar, and Amita Chandra. "Ion–Electron-Conducting Polymer Composites: Promising Electromagnetic Interference Shielding Material." *ACS Appl. Mater. Interfaces.* **2016**, 8, 18450-18461.
5. Z. Xiao-Juan et al. "Enhanced microwave absorption property of reduced graphene oxide (RGO)-$MnFe_2O_4$ nanocomposites and polyvinylidene fluoride." *ACS Appl. Mater. Interfaces*, **2014**, 6, 7471-7478.